

# Stacked-Residual PINN for State Reconstruction of Hyperbolic Systems

Katayoun Eshkofti and Matthieu Barreau

**Abstract**—In a more connected world, modeling multi-agent systems with hyperbolic partial differential equations (PDEs) offers a potential solution to the curse of dimensionality. However, classical control tools need adaptation for these complex systems. Physics-informed neural networks (PINNs) provide a powerful framework to fix this issue by inferring solutions to PDEs by embedding governing equations into the neural network. A major limitation of original PINNs is their inability to capture steep gradients and discontinuities in hyperbolic PDEs. This paper proposes a stacked residual PINN method enhanced with a vanishing viscosity mechanism. Initially, a basic PINN with a small viscosity coefficient provides a stable, low-fidelity solution. Residual correction blocks with learnable scaling parameters then iteratively refine this solution, progressively decreasing the viscosity coefficient to transition from parabolic to hyperbolic PDEs. Applying this method to traffic state reconstruction improved results by an order of magnitude in relative  $\mathcal{L}^2$  error, demonstrating its potential to accurately estimate solutions where original PINNs struggle with instability and low fidelity.

## I. INTRODUCTION

Quasi-linear Hyperbolic partial differential equations (PDEs) are crucial in modern control problems, emerging in a wide range of applications, from fluid dynamics to electrical energy transportation and traffic flow [1]. A notable example is the role of the Hamilton-Jacobi equation in optimal and predictive control, highlighting the ubiquity of hyperbolic PDEs across both physical modeling and abstract optimization applications in control theory. State reconstruction and identification of systems governed by hyperbolic PDEs is of fundamental interest, as it allows for estimating the complete evolution of the system from partial and noisy observations. This capability is key for monitoring distributed systems and enables subsequent control.

However, model identification and state reconstruction for quasi-linear hyperbolic PDEs are challenging due to their nonlinear dynamics, discontinuities, non-uniqueness, and infinite-dimensional nature. Traditional model-based approaches typically require precise knowledge of the system model, low dimensionality, and favorable theoretical conditions to guarantee convergence, which are often difficult to ensure for complex systems. On the other hand, commonly used machine learning methods [2] require a large number of measurements, which often results in overfitting [3].

These issues encourage the investigation of learning-based approaches that handle model uncertainties and efficiently

utilize data. To address this, the authors [4] introduced physics-informed neural networks (PINNs), integrating governing equations directly within neural networks. By embedding physical models into the loss function and penalizing deviations, PINNs effectively learn solutions from sparse and noisy data. Specifically, [5] demonstrated that PINNs simultaneously identify unknown model parameters, reconstruct traffic flow states from sparse vehicle data, and extend predictions. This reveals the potential of PINN-based approaches for state reconstruction in hyperbolic PDEs and serves as an incentive for the present research.

Since the original PINN development [4], recent modifications have improved performance in complex scenarios. For example, [6] proposed a multi-fidelity stacking approach, iteratively training a PINN to refine outputs progressively. Physics-informed residual adaptive networks employ projected input coordinates within residual blocks featuring adaptive skip connections to address deep multilayer perceptron derivative initialization issues [7]. Additionally, sequential and hierarchical PINN structures, such as multi-stage neural networks, have shown unique capabilities [8].

Although recent studies suggest PINNs outperform traditional deep learning methods [9], they have limitations, particularly for hyperbolic PDEs, where they struggle to capture sharp features like shocks or discontinuities [3]. Addressing these challenges motivates the development of more effective state estimation methods for hyperbolic PDEs. Moreover, no evidence demonstrates that PINN effectively learns the hyperbolic PDE underlying traffic state models with acceptable accuracy [3], making this an open and intriguing research area in traffic control.

Our contribution is to address this issue by utilizing limited measurements through an effective combination of vanishing viscosity from applied mathematics, curriculum learning from machine learning, and stacked PINNs. This approach ensures convergence to the correct hyperbolic limit, improving accuracy by an order of magnitude compared to the original PINN.

This paper consists of five sections. Section 2 reviews hyperbolic PDE formulations and the role of vanishing viscosity in ensuring stable, unique solutions. Section 3 introduces the stacked residual PINN methodology, outlining its architecture and training with decreasing viscosity. Section 4 presents numerical experiments on traffic state reconstruction, highlighting shock-capturing capabilities and comparing performance with the original PINN. Section 5 concludes with key findings and future research directions.

**Notation:** Let  $\mathbb{R}$  denote real numbers and  $\mathbb{R}^+$  nonnegative real numbers. For differentiable single-variable functions,

This work is partially supported by the Wallenberg AI, Autonomous Systems and Software Program (WASP) funded by the Knut and Alice Wallenberg Foundation and Digital Futures.

K. Eshkofti and M. Barreau are with the Division of Decision and Control Systems, Digital Futures, KTH Royal Institute of Technology, SE-100 44 Stockholm, Sweden {eshkofti,barreau}@kth.se

the prime notation  $f'$  represents derivatives. Multivariate functions' partial derivatives with respect to space and time are denoted by  $\partial f$  with corresponding subscripts. Moreover,  $C^1(\mathbb{R}^+ \times \mathbb{R})$  denotes continuously differentiable functions on the given domain.  $L^p(\Lambda)$  and  $H^k(\Lambda)$  represent Lebesgue and Sobolev spaces, respectively.  $L^\infty(\Lambda)$  consists of essentially bounded functions on  $\Lambda$ .

## II. BACKGROUND ON PROBLEM STATEMENT

The main goal of this paper is to find a solution  $u$  to the following 1d quasi-linear hyperbolic PDE posed on the spatiotemporal domain  $\Lambda = [0, T] \times [0, L] \subset \mathbb{R}^+ \times \mathbb{R}$ :

$$\begin{cases} \partial_t u + \partial_x f(u) = 0, & (t, x) \in \Lambda, \\ u(0, x) = u_0(x), & x \in [0, L], \\ u(t, 0) = u_b^-(t), \quad u(t, L) = u_b^+(t), & t \in [0, T]. \end{cases} \quad (1)$$

Here,  $u_0(x)$  and  $u_b^\pm(t)$  represent initial and boundary data, respectively. Additionally, suitable boundary conditions should be defined for the PDE in (1) to be well-posed [1]. It is assumed that  $f$  is a smooth flux function, at least  $f \in C^2(\mathbb{R})$ , so that the PDE is strictly hyperbolic. Moreover, to ensure that the mapping  $u \mapsto f(u)$  remains within  $H^1$  and to bound characteristic speeds, it is assumed that  $f$  is globally Lipschitz or has at most polynomial growth. Additionally, the initial data  $u_0$  is assumed to belong to a Sobolev space such as  $H^1(\Lambda)$  and to satisfy compatibility conditions with the boundary data.

Since hyperbolic solutions can develop discontinuities in finite time, we can only investigate weak solutions, which belong to a distribution space [1]. However, these weak solutions are not necessarily unique unless an entropy condition is imposed. A major theoretical challenge is therefore to prove the existence of weak entropic solutions. To this end, a convex entropy function  $\eta(u)$  is chosen, and an associated entropy flux  $q(u)$  is determined based on the compatibility condition outlined as  $q'(u) = \eta'(u)f'(u)$ .

A weak solution is then called entropy-admissible, provided that, in addition to satisfying the weak form of the conservation law, it also satisfies the entropy inequality ruled by  $\eta(u)_t + q(u)_x \leq 0$  in the sense of distributions. Under these conditions, often referred to as the Kruzkov entropy condition [10] in the scalar case or the Lax–Oleinik condition for nonlinear fluxes, weak solutions become unique and physically meaningful [11].

A more robust and practical way to construct weak entropy solutions is through the vanishing viscosity method. First, consider the parabolic regularization of (1), formulated as

$$\partial_t u_\gamma + \partial_x f(u_\gamma) = \gamma \partial_{xx} u_\gamma, \quad \gamma > 0. \quad (2)$$

where  $\gamma$  is a small viscosity coefficient. It is worth noting that the subscript  $u_\gamma$  signifies the solution corresponding to viscosity  $\gamma$ . Under the standard assumptions previously mentioned, the parabolic PDE in (2) results in a unique classical solution  $u_\gamma$  for each fixed  $\gamma$  [12, Theorem 14.6]. By finding estimates that are uniform with respect to  $\gamma$ , it is proved that the sequence  $\{u_\gamma\}$  remains bounded in

appropriate norms [11]. Uniform energy estimates and the derivation of an entropy inequality enable passing to the limit as  $\gamma \rightarrow 0$ , thereby, as discussed in Chapter 2 of [11], obtaining a weak solution that is entropy-admissible and satisfies the additional regularity conditions outlined as  $u \in C^0([0, T]; H^2([0, L])) \cap C^1([0, T]; H^1([0, L]))$ .

The rigorous justification of this limit passage and the well-posedness of the corresponding problem is established via a combination of compactness arguments and the construction of a basic quadratic Lyapunov function, as detailed in [1]. Moreover, the dissipativity of the boundary conditions is crucial to ensuring that the energy associated with the system decays over time. Consequently, by combining the vanishing viscosity method [10] with uniform energy and entropy estimates, the existence, uniqueness, and entropy admissibility of the solution to (1) are guaranteed.

**Problem:** We want to efficiently and accurately approximate the entropic solution  $u$  of a hyperbolic PDE specified in (1) using PINNs.

Although vanilla PINNs have been successfully applied to various types of problems, particularly those classified as parabolic PDEs in (2), a major limitation is their poor performance in terms of convergence and accuracy when solving hyperbolic PDEs governed by (1) [3]. In other words, PINNs fail to fully capture discontinuities and provide smooth solutions. Therefore, a modification to the PINN structure is necessary to enhance its ability to solve hyperbolic PDEs.

To achieve this objective, we introduce a novel variant of PINN called stacked residual PINN, which incrementally refines a baseline approximation through stacked residual-correction subnetworks. This approach incorporates both the PDE residual and data to enforce the governing equations while also guiding the solution in regions where the PDE may be insufficient or highly nonlinear.

In the following section, we demonstrate how adopting this smooth-to-sharp transition in the stacked residual PINN enhances the robustness of capturing discontinuities, enabling high-resolution reconstruction of hyperbolic PDE states.

## III. METHODOLOGY

This paper proposes the stacked residual PINN to solve the hyperbolic PDEs discussed in Section 3. First, an overview of the proposed architecture is presented, followed by a detailed discussion of its application to hyperbolic PDEs.

### A. Classical PINN

In the standard formulation of PINNs, the goal is to approximate the solution  $u$  of PDE (1) using a dense feedforward neural network  $\hat{u}(\cdot; \theta)$ . Let the neural network have  $L$  hidden layers, formulated as follows:

$$\begin{aligned} \hat{u}(t, x; \theta) &= W_L \times H_{L-1} \circ \cdots \circ H_1(t, x) + b_L \\ &\triangleq \mathcal{N}([t, x]; \theta), \end{aligned} \quad (3)$$

for  $(t, x) \in \Lambda$  where  $(t, x)$  represents the input coordinates in the spatiotemporal domain. For each hidden layer  $l = 1, \dots, L-1$ , the feature map is defined as:

$$H_l(t, x) = \phi(W_l H_{l-1}(t, x) + b_l). \quad (4)$$

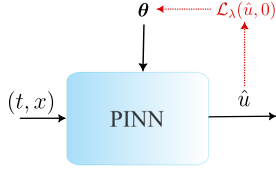


Fig. 1: Vanilla PINN structure. Black lines are forwardpass and red-dotted lines are backpropagation.

Here  $H_0(t, x) = [t \ x]^\top$ . Moreover,  $W_l \in \mathbb{R}^{n_l \times n_{l-1}}$  and  $b_l \in \mathbb{R}^{n_l}$  represent the weight matrices and bias vectors at layer  $l$ . The entire set of network parameters denoted by  $\theta = \{W_l, b_l\}_{l=1}^L$  and the activation function is  $\phi \in C^\infty(\mathbb{R}, \mathbb{R})$ .

We are interested in approximating the unique entropic solution  $u$  to (1), meaning that we want to solve the following constrained optimization problem:

$$\begin{aligned} \theta^* = \operatorname{Argmin}_{\theta} \quad & \int_{\Gamma} \|u(\nu) - \hat{u}(\nu)\|^2 d\nu \\ \text{s. t.} \quad & \int_{\Lambda} |r_0(\cdot; \hat{u}(\cdot; \theta))|^2 = 0, \end{aligned}$$

where  $\Gamma = \Gamma_{init} \cup \Gamma_{boundary}$  is the measured boundary of System (1) with

$$\begin{aligned} \Gamma_{init} &= \{(0, x) \mid x \in [0, L]\}, \\ \Gamma_{boundary} &= \{(t, 0) \mid t \in [0, T]\} \cup \{(t, L) \mid t \in [0, T]\}, \end{aligned}$$

and  $\hat{u}$  refers to  $\hat{u}(\cdot, \theta)$  to ease the reading. The residual  $r$  is also defined as:

$$r_\gamma(\cdot; \hat{u}) = \partial_t \hat{u} + \partial_x f(\hat{u}) - \gamma \partial_{xx} \hat{u}. \quad (5)$$

The previous problem cannot be numerically solved because it contains integrals. Following the methodology in [13] using Monte-Carlo sampling and the Lagrangian formulation, we get the following relaxed but numerically tractable optimization problem:

$$\theta^* = \operatorname{Argmin}_{\theta} \max_{\lambda > 0} \mathcal{L}_\lambda(\hat{u}, \gamma),$$

where  $\mathcal{L}_\lambda(\hat{u}, \gamma) = \mathcal{L}_{data}(\hat{u}(\cdot, \theta)) + \lambda \mathcal{L}_{phy}(\hat{u}(\cdot, \theta), 0)$ .

$$\mathcal{L}_{data}(\hat{u}) = \frac{1}{|\mathcal{D}_{data}|} \sum_{(t,x) \in \mathcal{D}_{data}} |u(t, x) - \hat{u}(t, x)|^2,$$

$$\mathcal{L}_{phy}(\hat{u}, \gamma) = \frac{1}{|\mathcal{D}_{phy}|} \sum_{(t,x) \in \mathcal{D}_{phy}} |r_\gamma(t, x; \hat{u})|^2,$$

with  $\mathcal{D}_{phy} \subset \Lambda$  a discrete set of cardinal  $|\mathcal{D}_{phy}|$  and  $\mathcal{D}_{data} \subset \Gamma$  a discrete set of cardinal  $|\mathcal{D}_{data}|$ . This problem is typically solved using a primal-dual strategy, alternating between gradient descent on the min problem over the tensor of parameters  $\theta$  and the max over the Lagrange multiplier  $\lambda$ . A simpler and often efficient method is to fix  $\lambda$  to a small constant and apply gradient descent only to the min problem. For simplicity, we consider this option in this paper.

The total loss function consists then of two terms: the data mismatch  $\mathcal{L}_{data}$  and the PDE residual  $\mathcal{L}_{phy}$ . These losses are computed using the mean square error between the true and the approximated solution, making the optimization problem a learning one. For the physics loss, we want to minimize the PDE residual  $r_\gamma(\cdot; \theta)$  over  $\Lambda$ , bringing regularization and

forcing the convergence to the solution of the PDE. The general structure of PINN is illustrated in Fig. 1.

As explained in [13], [14], the PINN methodology only succeeds in the case of a Lipschitz continuous PDE operator, which is never the case in hyperbolic problems such as (1). The following section provides a detailed discussion of a refined architecture that proposes a solution.

## B. Residual PINN

First, consider solving the regularized PDE in (2). If  $\gamma$  is small enough, then the approximated solution will be close to the entropic solution of (1), based on the vanishing viscosity method [10]. To this end, the initial stage consists of a baseline PINN designed to approximate the solution  $u_{\gamma_{init}}$  to the parabolic PDE (2) by  $\hat{u}^{(0)}(\cdot; \theta_0)$ . At this stage, the viscosity coefficient  $\gamma_{init}$  is chosen to be large enough to ensure that  $\hat{u}$  is entropic and that the PDE operator is sufficiently Lipschitz to guarantee that the PINN can successfully learn the approximated solution.

One key idea of this article is to combine the vanishing methodology with the residual-network architecture [15]. Subsequently, we introduce a residual stage where  $\hat{u}^{(0)}$  is refined by a single residual correction network to get  $\hat{u}^{(1)}$ , as shown in Fig. 2. This residual-correction PINN bears a close resemblance to a Luenberger observer that feedbacks the difference  $u - \hat{u}$  to update its estimate. In both cases, the discrepancy triggers the correction. At this stage, the viscosity coefficient is  $\gamma_1 = 0$ , hence the solution to the hyperbolic PDE in (1) is approximated by  $\hat{u}^{(1)}$ . Consequently, the solution approximation at the second stage is:

$$\hat{u}^{(1)}(t, x; \theta_1) = \hat{u}^{(0)}(t, x; \theta_0) + |\alpha_1| \mathcal{N}([t, x, \hat{u}^{(0)}(t, x)]; \theta_1). \quad (6)$$

In practice, the residual block is a feedforward neural network whose inputs include the spatiotemporal coordinates  $(t, x)$  and the approximation at the previous step  $\hat{u}^{(0)}(t, x)$ . Moreover,  $|\alpha_1|$  is a learnable scaling parameter that determines and controls the extent to which each residual block contributes to the update. The new optimization problem is

$$\theta_0^*, \theta_1^* = \operatorname{Argmin}_{\theta_0, \theta_1} \mathcal{L}_{res}(\theta_0, \theta_1) + \alpha_1^2,$$

where

$$\mathcal{L}_{res}(\theta_0, \theta_1) = \frac{1}{2} \left( \mathcal{L}_\lambda(\hat{u}^{(0)}, \gamma_{init}) + \mathcal{L}_\lambda(\hat{u}^{(1)}, 0) \right).$$

As discussed in Section 2, the vanishing viscosity principle ensures that the solution to the parabolic PDE in (2), with a small viscosity term, converges to the entropic weak solution to the corresponding hyperbolic PDE as the viscosity coefficient decreases to zero. For instance, in the case of the Burgers equation, the Cole–Hopf transformation reveals that  $u_\gamma$  changes smoothly with viscosity  $\gamma$  to converge asymptotically to the solution to the hyperbolic system. This justifies that the same applies here. The coefficient  $\alpha_1$  is introduced because we want to keep the correction small that we only correct slightly the parabolic solution, ensuring that the hyperbolic solution remains entropic. Indeed, a large

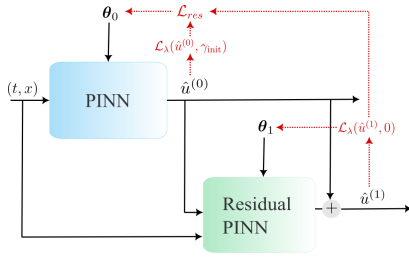


Fig. 2: Residual PINN structure. Black lines are forwardpass and red-dotted lines are backpropagation.

$\alpha_1$  will probably signify that  $\hat{u}^{(1)}$  is quite different from  $\hat{u}^{(0)}$  which does not align with the vanishing viscosity method.

As a result, training a PINN on the parabolic form in the initial stage, which admits a unique smooth solution, and then transitioning to the hyperbolic PDE allows for acquiring both the stability of the parabolic regime and the fidelity of the hyperbolic limit.

### C. Stacked residual PINN and vanishing viscosity approach

While a single residual correction block may succeed in simple problems, it can fail when dealing with sharp and localized solution features. Moreover, relying on a single residual PINN to approximate both smooth regions and shocks imposes a burden on the learning process.

The other key idea of this article is to adapt the iterative stacking method put forward by [6]. In our study, by stacking multiple residual blocks, each trained with a successively smaller  $\gamma$ , a multi-stage correction process is implemented following the vanishing viscosity method. In fact, each stage leverages the well-posedness of the parabolic PDE in (2) to compute a smooth and stable correction, which is then gradually refined to capture the sharper features of the hyperbolic PDEs. In other words,  $\hat{u}^{(0)}$  is incrementally refined by stacking  $n$  residual-correction subnetworks. The approximation at the  $i$ th stage is given by:

$$\hat{u}^{(i)}(t, x; \theta_i) = \hat{u}^{(i-1)}(t, x; \theta_{i-1}) + |\alpha_i| \mathcal{N}([t, x, \hat{u}^{(i-1)}(t, x)]; \theta_i). \quad (7)$$

where  $i \in \{1, \dots, n\}$ . The parameter  $\gamma_i$  is a monotonically decreasing function of the residual layer, for instance:

$$\gamma_i = \gamma_{\text{init}} \left[ 1 - \left( \frac{i}{n} \right)^p \right], \quad (8)$$

so that  $\gamma_0 = \gamma_{\text{init}} > 0$  and  $\gamma_n = 0$ . As in the viscous Burgers equation, the Cole–Hopf transform demonstrates that solutions depend exponentially on the viscosity parameter. As  $\gamma$  decreases, the transformed solution exhibits rapid exponential changes. Therefore, integrating a superlinear  $\gamma$ , as outlined in (8) with  $p > 1$ , ensures that the stacked residual blocks smoothly capture the transition from parabolic to hyperbolic behavior without compromising stability.

As in stage 1, a physics-informed loss is imposed at each level  $i$ , ensuring that  $r_{\gamma_i}(\cdot; \theta_i)$  remains small along with the usual boundary and initial conditions. In other words,

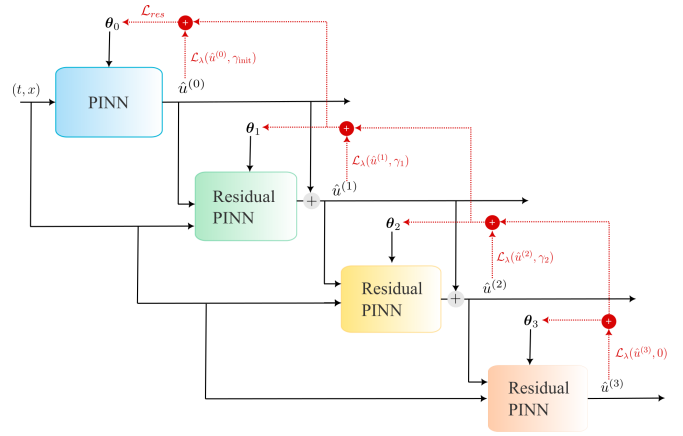


Fig. 3: Stacked residual PINN. Black lines are forwardpass and red-dotted lines are backpropagation.

at stacked residual block  $i$ , the PDE residual is governed by  $r_{\gamma_i}$  such that the first block gets the viscous coefficient  $\gamma_{\text{init}}$  and the last stage  $\gamma_n = 0$ . The optimization problem can be formulated as:

$$\{\theta_i^*\}_{i=0}^n = \text{Argmin}_{\{\theta_i\}_{i=0}^n} \mathcal{L}_{\text{stacked}}(\{\theta_i\}_{i=0}^n) + \sum_{i=1}^n \alpha_i^2$$

where

$$\mathcal{L}_{\text{stacked}}(\{\theta_i\}_{i=0}^n) = \frac{1}{n+1} \sum_{i=0}^n \mathcal{L}_{\lambda}(\hat{u}^{(i)}, \gamma_i).$$

Here  $\mathcal{L}_{\text{stacked}}$  represents the total loss function, which consists of the base PINN and the stacked residual PINNs. The residual PINN block diagram is presented in Figure 3.

*Remark 1:* The stacked PINN method was initially introduced in [6], where they employed a multi-fidelity strategy that stacks PINNs. In this approach, each network’s output provides a lower-fidelity input for the next stage, incrementally refining the model’s expressivity.

We share the same idea; however, our method employs a residual PINN at each stage. Contrary to [6], we use a different residual  $r_{\gamma}$  at each stage to align with the vanishing viscosity method.  $\blacklozenge$

With this approach, we obtain certain convergence guarantees, as stated in the following proposition.

*Proposition 1:* Consider the hyperbolic PDE in (1) with an entropy-entropy flux pair  $(\eta(u), q(u))$ , satisfying the entropy condition  $\eta''(u) \geq 0$  and  $q'(u) = \eta'(u)f'(u)$ . Let  $\gamma_{\text{init}} > 0$  and consider a sequence of viscosity coefficients defined as in (8), ensuring  $\gamma_n = 0$ . Assume the following:

- 1) For each  $\gamma_i > 0$ , the parabolic PDE in (2) admits a unique smooth solution  $u_{\gamma_i}$ , converging strongly in  $L^1(\Lambda)$  to the entropy solution of  $u$  in (1) as  $\gamma_i \rightarrow 0$ .
- 2) Based on universal approximation [16], at each stage  $i$ , the neural network  $\hat{u}^{(i)}(\cdot, \theta_i)$  has sufficient expressivity such that with the error bounded by  $\varepsilon_i$ , that is:

$$\|\hat{u}^{(i)} - u_{\gamma_i}\|_{L^2(\Lambda)} \leq \varepsilon_i, \quad \text{where } \varepsilon_i \rightarrow 0 \text{ as } i \rightarrow n.$$

Then, the stacked residual PINN solution  $\hat{u}^{(n)}$  converges to the entropy solution of (1). In other words,

$$\lim_{n \rightarrow \infty} \|\hat{u}^{(n)} - u\|_{L^1(\Lambda)} = 0.$$

*Proof:* According to the vanishing viscosity theorem [10], for the sequence  $\{\gamma_i\}$  with  $\gamma_i \rightarrow 0$  as  $i \rightarrow n$ , we have  $\lim_{i \rightarrow n} \|u_{\gamma_i} - u\|_{L^1(\mathcal{D})} = 0$ .

Considering the second assumption, the residual correction mechanism ensures that the discrepancy between  $\hat{u}^{(i)}$  and the viscous solution  $u_{\gamma_i}$  is minimized through the physics loss  $\mathcal{L}_{\text{phy}}(\gamma_i, \hat{u}^{(i)})$ . The total error at stage  $i$  decomposes as:

$$\|\hat{u}^{(i)} - u\|^2 \leq \underbrace{\|\hat{u}^{(i)} - u_{\gamma_i}\|^2}_{\varepsilon_i} + \underbrace{\|u_{\gamma_i} - u\|^2}_{\delta_i}.$$

By the first assumption,  $\delta_i \rightarrow 0$  as  $\gamma_i \rightarrow 0$ . By the second assumption, with a sufficiently large network,  $\varepsilon_i \rightarrow 0$ . For the sequence  $\{\hat{u}^{(i)}\}$ , we have

$$\|\hat{u}^{(n)} - u\| \leq \sum_{i=0}^n \varepsilon_i + \sum_{i=0}^n \delta_i.$$

Since both series converge under assumptions 1 and 2, the proof is complete. ■

#### IV. RESULTS

In this section, our goal is to estimate vehicle density over a road  $[0, L]$  from local density measurements by employing the proposed stacked residual PINN<sup>1</sup>.

In the example considered, the PDE (1) represents the LWR model [17], [18]. The normalized density  $u$  is defined such that  $u = 0$  corresponds to an empty road, while  $u = 1$  represents bumper-to-bumper traffic conditions. Two density measurements are provided at the boundaries  $x \in \{0, L\}$  and can be collected using loop detectors.

Additionally,  $f(u) = V_f u(1 - u)$  is referred to as the Greenshields flow equation [19], which describes the relationship between vehicle velocity and density. The parameter  $V_f$  denotes the free-flow velocity. The Greenshields function serves as the advection term, and its nonlinear dependence on  $u$  can lead to shock formation or discontinuities.

By employing the vanishing viscosity limit, the governing equation in (2) is considered, and a small initial viscosity coefficient  $\gamma_{\text{init}} = 0.1$ . To investigate the impact of stacked layers on the improvement of results, the algorithm is implemented while considering four different numbers of stacked residual blocks,  $n = \{0, 1, 3, 5\}$ , where  $n = 0$  represents vanilla PINN. To compute data loss (i.e.,  $\mathcal{L}_{\text{data}}$ ) in the total loss function of PINN, density measurements are supplied via Godunov simulation of (1).

The baseline PINN at the initial stage consists of three hidden layers, each with 30 neurons. Each residual correction block comprises three hidden layers, each with 40 neurons. Vanishing viscosity is implemented via the function defined in (8), where  $p = 2$ .

<sup>1</sup>The code and data are available at <https://github.com/KatayounEshkofti/StackedResidualPINN>

# Stacked residual blocks	0	1	3	5
Relative $\mathcal{L}^2$ error ( $\times 10^{-2}$ )	18.98	13.86	4.86	4.66

TABLE I: Relative  $\mathcal{L}^2$  error for various numbers of stacked residual blocks.

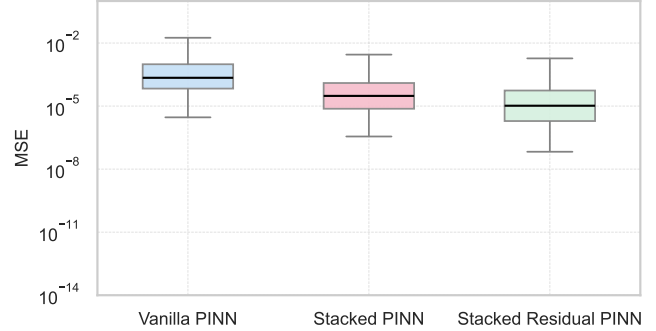


Fig. 4: Comparison of  $\mathcal{L}^2$ -error of three methods in traffic reconstruction problem.

It is worth noting that, to ensure a fair comparison across all scenarios, the same number of hidden layers and neurons is utilized. Additionally, the number of training iterations for Adam is set to 15,000 for all scenarios.

The results are compared with solutions obtained from the Godunov simulation, and the relative  $\mathcal{L}^2$  error is defined as the evaluation metric:

$$\text{relative } \mathcal{L}^2 = \frac{\|u - \hat{u}\|_2}{\|u\|_2}. \quad (9)$$

The relative  $\mathcal{L}^2$  error quantifies the percentage discrepancy between the estimated density and exact values. As shown in Table I, increasing stacked residual blocks from 0 to 5 consistently reduces the error from about 19% to 4%. This suggests that additional residual blocks enhance estimation accuracy, though the smaller gain from 3 to 5 blocks may indicate diminishing returns.

Moreover, to compare our proposed method with the stacked PINN developed by [6] and the original PINN, the box plot of the  $\mathcal{L}^2$ -error for these methods is shown in Fig. 4. Note that the modified stacked PINN [6] integrates vanishing viscosity into stacked networks. Both stacked PINN and stacked residual PINN consist of three stacked networks, each with three hidden layers and 40 neurons. For fairness, the vanilla PINN consists of nine hidden layers, each with 40 neurons. As shown in Figure 4, the stacked residual PINN achieves the lowest  $\mathcal{L}^2$ -error, improving accuracy by an order of magnitude compared to the vanilla PINN. The accuracy of the proposed method can be seen from Fig. 5 where all shocks are correctly positioned. More specifically, Fig. 6 shows that the first residual block  $\alpha_1 \mathcal{N}(\cdot, \theta_1)$  is far from being zero, indicating that it is grasping more shocks and sharpening the existing ones from the previous block.

These results indicate that progressively stacking networks enhances reconstruction accuracy, while residual correction networks further stabilize learning, leading to lower errors and reduced variability in state estimations.



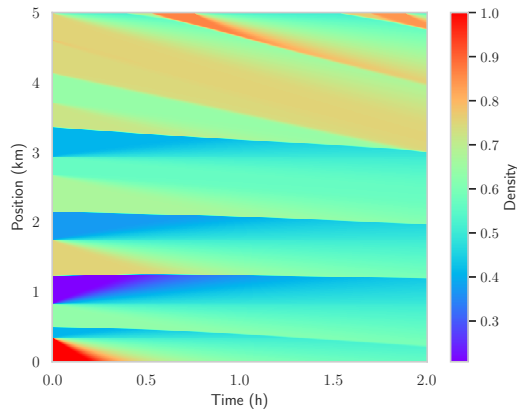
## V. CONCLUSION AND FUTURE WORKS

This paper introduced the stacked residual PINN, a variation of the PINN framework designed to reconstruct states of hyperbolic PDEs. By adopting the vanishing viscosity principle, the approach progressively enhances solution approximation, effectively capturing discontinuities and shocks. Applied to a traffic state reconstruction problem, the method demonstrated an order of magnitude improvement in accuracy over the vanilla PINN.

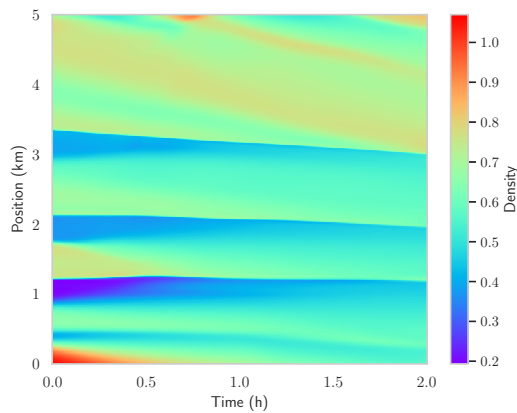
Future work will focus on extending the methodology to higher-dimensional and more complex hyperbolic PDEs, aiming to confirm its broader applicability, particularly in control engineering.

## REFERENCES

- [1] G. Bastin and J.-M. Coron, *Stability and Boundary Stabilization of 1-D Hyperbolic Systems*. Birkhäuser Cham, 2016.
- [2] N. G. Polson and V. O. Sokolov, "Deep learning for short-term traffic flow prediction," *Transportation Research Part C: Emerging Technologies*, 2017.
- [3] A. J. Huang and S. Agarwal, "On the limitations of physics-informed deep learning: Illustrations using first-order hyperbolic conservation law-based traffic flow models," *IEEE Open Journal of Intelligent Transportation Systems*, 2023.
- [4] M. Raissi, P. Perdikaris, and G. E. Karniadakis, "Physics-informed neural networks: A deep learning framework for solving forward and inverse problems involving nonlinear partial differential equations," *Journal of Computational Physics*, 2019.
- [5] M. Barreau, M. Aguiar, J. Liu, and K. H. Johansson, "Physics-informed learning for identification and state reconstruction of traffic density," in *60th IEEE Conference on Decision and Control*, 2021.
- [6] A. A. Howard, S. H. Murphy, and al., "Stacked networks improve physics-informed training: Applications to neural networks and deep operator networks," *Foundations of Data Science*, 2025.
- [7] S. Wang, B. Li, Y. Chen, and P. Perdikaris, "Piratenets: Physics-informed deep learning with residual adaptive networks," *Journal of Machine Learning Research*, 2025.
- [8] Y. Wang and C.-Y. Lai, "Multi-stage neural networks: Function approximator of machine precision," *Journal of Computational Physics*, 2024.
- [9] A. J. Huang and S. Agarwal, "Physics informed deep learning for traffic state estimation," in *2020 IEEE 23rd International Conference on Intelligent Transportation Systems (ITSC)*, 2020.
- [10] S. N. Kružkov, "First order quasilinear equations in several independent variables," *Mathematics of the USSR-Sbornik*, 1970.
- [11] C. M. Dafermos, *Hyperbolic Conservation Laws in Continuum Physics*. Springer Berlin, Heidelberg, 2016.
- [12] H. Amann, "Nonhomogeneous linear and quasilinear elliptic and parabolic boundary value problems," in *Function spaces, differential operators and nonlinear analysis*. Springer, 1993.
- [13] M. Barreau and H. Shen, "Accuracy and robustness of weight-balancing methods for training PINNs," *Arxiv*, 2025.
- [14] J. Sirignano and K. Spiliopoulos, "DGM: A deep learning algorithm for solving partial differential equations," *Journal of computational physics*, 2018.
- [15] K. He, X. Zhang, S. Ren, and J. Sun, "Deep residual learning for image recognition," in *Proceedings of the IEEE conference on computer vision and pattern recognition*, 2016.
- [16] K. Hornik, "Approximation capabilities of multilayer feedforward networks," *Neural networks*, 1991.
- [17] P. I. Richards, "Shock waves on the highway," *Operations Research*, 1956.
- [18] M. J. Lighthill and G. B. Whitham, "On kinematic waves II. a theory of traffic flow on long crowded roads," *Proceedings of the Royal Society of London. Series A. Mathematical and Physical Sciences*, 1955.
- [19] B. D. Greenshields, J. R. Bibbins, W. S. Channing, and H. H. Miller, "A study of traffic capacity," in *Highway research board proceedings*, 1935.



(a)  $u$



(b)  $\hat{u}^{(3)}$

Fig. 5: Numerical examples on the state reconstruction.

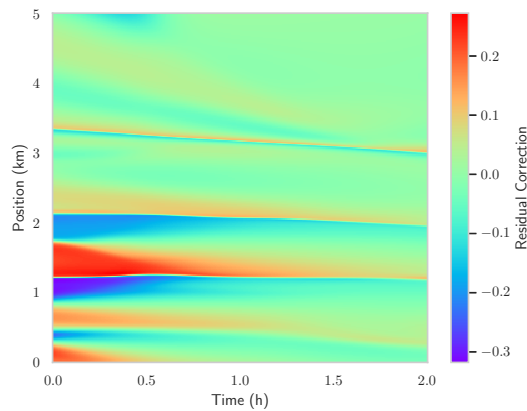


Fig. 6: Value of the residual block  $\alpha_1 \mathcal{N}(\cdot; \theta_1)$ .